Available online at www.sciencedirect.com

ScienceDirect

Energy Procedia 80 (2015) 442 – 449

Energy Procedia

EERA DeepWind'2015, 12th Deep Sea Offshore Wind R&D Conference

Isogeometric methods for CFD and FSI-simulation of flow around turbine blades

Timo van Opstal[a], Eivind Fonn[b], Runar Holdahl[c], Trond Kvamsdal[a,b], Arne Morten Kvarving[b], Kjell Magne Mathisen[d], Knut Nordanger[a], Knut Morten Okstad[b], Adil Rasheed[b], Mandar Tabib[b]

[a]*Mathematical Sciences, NTNU, Alfred Getz vei 1, 7491, Trondheim*
[b]*Applied Mathematics, SINTEF ICT, Strindvegen 4, 7034, Trondheim*
[c]*Statoil, Pb 1176 Sentrum, 0107 Oslo*
[d]*Structural Engineering, NTNU, Richard Birkelands vei 1, 7491, Trondheim*

Abstract

Coupled fluid-structure interaction simulations of wind turbines have traditionally been considered computationally too expensive to carry out. However, more powerful computers and better solution techniques based on IsoGeometric Analysis (IGA) can make such simulations viable. Literature indicates that the smoothness of IGA approximations generally yield higher accuracy per-degree-of-freedom. We consider a two-dimensional test case prototypical of wake-vortex analyses and strip-theory approaches used in the numerical simulation of wind turbine.

Peer-review under responsibility of SINTEF Energi AS
Keywords: Isogeometric Analysis; Finite Element method; Wind turbine blades

1. Introduction

Wind turbines can establish themself as an important source of renewable energy if increased power output and reduced installation and maintainence costs can be realized. To increase power output rotor diameters are increased and wind parks are being moved offshore. These combined trends fundamentally change the operating conditions at which such turbines are expected to produce power. On account of the strong winds and wind variations and long, flexible blades Fluid-Structure Interaction (FSI) with large deformations must be taken into account to be able to accurately predict such destructive phenomena as flutter and buckling.

On the other hand, such simulations have traditionally been considered computationally too expensive to carry out. The advance of both hardware and solution techniques have however given new impulse to this endeavor. In particular

E-mail address: timo.vanopstal@math.ntnu.no

Peer-review under responsibility of SINTEF Energi AS
doi:10.1016/j.egypro.2015.11.448

Hsu, Bazilevs and coworkers [1–3], have pioneered full FSI computations of the full wind turbine (rotor, nacelle and tower) using an ALE-VMS method.

There is a continued demand to bring this kind of wind turbine analyses within reach of industrial practice. More efficient techniques, building on the broad framework layed out in [1,2], need to be explored. A number of complementary techniques have been explored in this context. Since representative Reynolds numbers can reach 10^6–10^7, turbulence modeling is a vital ingredient. The Variational MultiScale (VMS) and Reynolds-Averaged Navier-Stokes (RANS) methods have been considered and contrasted [4,5]. Also, a *strip theory* approach, in which the flow is computed at planes intersecting the structure, is explored in [6]. Projection methods have been observed to perform well in [5]. Here we consider the use of IGA.

IGA is a technology rendering CAD representations suitable for numerical analysis. One important goal is to avoid or mitigate any mesh generation efforts. Direct use of the CAD representation implies that any geometrical approximation error is eliminated in the analysis model. In design, smooth geometries have been a key requirement from the onset, and inheriting this higher smoothness (and polynomial order) through the isoparametric concept has incidentally led to highly accurate numerical approximations. The gain obtained by high regularity and order are an active area of research, cf. e.g. [7], and is dependent on the mathematical model under consideration. For CFD, the gain of IGA has been investigated in, e.g. [4,5,8]. The higher smoothness has also paved the way for div-compatible discretizations. Exact satisfaction of the incompressibility constraint greatly improves accuracy, even on very coarse meshes [9,10]. These indications encourage the exploration of IGA in the context of wind turbines.

In this contribution we consider a Spalart-Almaras turbulence model, which is expected to perform well for bluff bodies and largely attached flow. The pitching airfoil at high Reynolds number, which exhibits many of the challenging flow phenomena in wind turbine simulations, is simulated. In this case the flow regime is comparable to that of the application, some flow separation is expected, and there are considerable deformations of the fluid domain. In this setting the value of employing IGA is investigated.

This paper is structured as follows. In §2, the mathematical model, its isogeometric discretization and numerical solution are treated. In §3 the test case is introduced and the numerical results analyzed. Finally, conclusions are drawn in §4.

2. Modeling, discretization and solution

In this section the physical model and the derived discrete model are presented. First, the governing equations for incompressible flow with Reynolds-averaged turbulence modeling are given in §2.1. Then, its discretization into a general finite element framework is elaborated in §2.2. Continuing, the isogeometric approach used in this finite element context is detailed in §2.3. Finally, we conclude with a note on time-discretization and on solution techniques §§2.4-2.5.

2.1. Reynolds-averaged Navier-Stokes with a Spalart-Almaras closure model

We consider a time interval $(0, T)$ and a reference domain Ω_0. The domain of the problem is the time-dependent current domain Ω_t, which may change on account of the movement of the embedded structure. We denote its boundary by $\partial\Omega_t$. It is the disjoint union of Γ_D, where Dirichlet boundary conditions apply, and and Γ_N, where Neumann boundary conditions apply.[1] The motion is given through a displacement field d over Ω_0. Given an initial velocity field u_0; a body force f and dynamic viscosity μ, a velocity pressure pair (u, p) is sought, that satisfies the Arbitrary

[1] Note that it is possible to prescribe combinations of Dirichlet and Neumann conditions in linearly independent directions, for instance, the *slip* condition $u \cdot n = 0 = t \cdot \partial_n\sigma \; \forall t \perp n$.

Lagrangian-Eulerian (ALE) formulation of the Navier-Stokes equations,

$$\partial_t u + (u - \partial_t d) \cdot \nabla u - \nabla \cdot \sigma(u, p) = f \text{ in } \Omega_t, \tag{1a}$$
$$\nabla \cdot u = 0 \text{ in } \Omega_t, \tag{1b}$$
$$u = g \text{ in } \Gamma_D, \tag{1c}$$
$$\partial_n \sigma(u, p) = h \text{ in } \Gamma_N, \tag{1d}$$
$$u(0) = u_0 \text{ in } \Omega_0. \tag{1e}$$

In these equations ∂_t denotes a time derivative, $\partial_t d$ the so-called *grid velocity*, $\sigma(u, p) := \mu\epsilon(u) - p$ is the Newtonian stress and $u(0)$ is the trace of u at $\{0\} \times \Omega$. Furthermore, $\epsilon(u) := \nabla u + (\nabla u)^\top$. Moreover, we assume that u_0 satisfies (1b) and (1c).

The grid movement is an artificial field that should minimize mesh distortion, especially in the sensitive boundary-layer region. In this work we consider linear elasticity to govern this displacement field:

$$\nabla_0 \cdot (FS) = 0 \text{ in } \Omega$$

with $F = \nabla_0 d$ the deformation gradient, $J = \det F$, $S = JF^{-1}\varsigma F^{-\top}$ the second Piola tensor and $\varsigma = 2\mu\epsilon(d) + \lambda(\text{tr}\epsilon(d))I$ Cauchy's stress tensor. Spatial derivatives with respect to the reference are denoted ∇_0. The Lamé parameters (λ, μ) are chosen to be high close to solid boundaries and to decay exponentially.

In the turbulent regime the above system becomes less tractable to solve as turbulent features of *small* spatio-temporal scales emerge. As highlighted in the introduction, the present approach to this conundrum is to model the effect of features of these small scales. The analyst defines the term small, i.e., which features are to be captured by a model though the spatio-temporal resolution of the discretization. We presently consider RANS, where turbulence is modeled by an *unknown* effective eddy viscosity ν_t, which replaces the *known* parameter ν in (1). This eddy viscosity is defined through

$$\nu_t = \tilde{\nu} f_{\nu 1}, \qquad f_{\nu 1} = \frac{\chi^3}{\chi^3 + c_{\nu 3}^3}, \qquad \chi = \frac{\tilde{\nu}}{\nu}. \tag{2}$$

The system is then closed with a transport equation for $\tilde{\nu}$, the *S-A model*, [11]

$$\partial_t \tilde{\nu} + u \cdot \nabla \tilde{\nu} - P(\tilde{\nu}) + D(\tilde{\nu}, \tilde{S}) + A(\tilde{\nu}) = 0 \text{ in } [0, T] \times \Omega, \tag{3a}$$
$$\tilde{\nu}(0) = \nu_0 \text{ in } \Omega, \tag{3b}$$
$$\tilde{\nu} = \nu_0 \text{ in } [0, T] \times \Gamma_I, \tag{3c}$$
$$\tilde{\nu} = 0 \text{ in } [0, T] \times \Gamma_W. \tag{3d}$$

In these equations, P, D and A represent production, wall dissipation and auxilliary forcing terms respectively. The modified vorticity is denoted $\tilde{S} = \tilde{S}(|\nabla \times u|, \tilde{\nu})$. Also, $\Gamma_I := \text{supp}(g)$ and $\Gamma_W := \Gamma_D - \Gamma_I$ represent the inflow and wall boundaries. The initial value $\nu_0 : \Omega \to \mathbb{R}$ is generally selected to be 5ν, which renders (3b) and (3d) incompatible. This is resolved by redefining ν_0 to retain the value 5ν everywhere outside a neighborhood of Γ_W where it smoothly decays to zero to satisfy (3d). This is of little consequence, as the definition of ν_0 should not affect the result, as long as it is *reasonable*. It is beyond the scope of this discussion to give a complete definition of the S-A model and its several modifications, the interested reader is referred to [12] for further details.

2.2. Finite elements

Numerical approximation of the above system requires stabilization, which is defined in terms of the discrezation. To this end we introduce a tesselation $\mathcal{T}^h$ of the domain Ω into elements K such that $\overline{\cup_{K \in \mathcal{T}^h} K} = \Omega$, where h is some measure of the resolution of $\mathcal{T}^h$.

Discretization by the FEM departs from a variational form obtained by multiplying the equations (1) and (3a) by test functions and integrating by parts. This yields the problem:

for all $t \in [0, T]$, find $(u - u_0, p, \tilde{\nu} - \nu_0) \in V \times Q \times M$ such that for all $(v, q, m) \in V \times Q \times M$:

$$B((u, p, \tilde{\nu}); (v, q, m)) = F((v, q, m)) \tag{4}$$

with $B((u, p, \tilde{\nu}); (v, q, m)) = B_{NS}|_{\nu}((u, p), (v, q)) + B_{SA}|_{u}(\tilde{\nu}, m)$ where the restriction operator $|_{(\cdot)}$ communicates the dependence with respect to $(\cdot)$ but implying that it plays the role of data. Also V, Q and M denote suitable vector spaces in which the solution is sought. In the following, $(\cdot, \cdot)$ denotes the $L^2(\Omega)$ inner product.

$$\begin{aligned}
B_{NS}|_{\nu}((u, p); (v, q)) &:= (\partial_t u, v) + (u \cdot \nabla u, v) + (\nu \nabla u, \nabla v) - (p, \nabla v) - (q, \nabla u),\\
B_{SA}|_{u}(\tilde{\nu}, m) &:= (\partial_t \tilde{\nu}, m) + (u \cdot \nabla \tilde{\nu}, m) - (P(\tilde{\nu}), m)\\
&\quad + (D(\tilde{\nu}, \tilde{S}), m) + (A(\tilde{\nu}), m),\\
F((v, q, m)) &:= (f, v) + \int_{\Gamma_N} hv.
\end{aligned}$$

The stream-wise resolution does not contribute much to the accuracy of the results because of the averaging procedure in the RANS and the self-similarity of the flow in this direction. Sacrificing this resolution requires stabilization due to high local CFL numbers and Streamline Upwind/Petrov-Galerkin stabilization (SUPG) [13] is selected for this purpose. In addition, an equal order interpolation will be used, so Pressure Stabilization/Petrov-Galerkin (PSPG) [14] is used. Denoting the residual of the momentum equation (1a) as $r_M(u, p) := \partial_t u + u \cdot \nabla u - \nabla \cdot \sigma(u, p) - f$, the stabilization terms, to be added to the bilinear form B, read

$$B_{stab,M}((u, p); (v, q)) := \sum_{K \in \mathcal{T}^h} (\tau_M r_M(u, p), u \cdot \nabla v + \nabla q)_K,$$

where $(\cdot, \cdot)_K$ is the $L^2(K)$ inner product and τ_M is the stabilization parameter. Moreover, denoting the residual of the Spalart-Allmaras equation (3a) as $r_S(\tilde{\nu}, u) := \partial_t \tilde{\nu} + u \cdot \nabla \tilde{\nu} - P(\tilde{\nu}) + D(\tilde{\nu}, \tilde{S}) + A(\tilde{\nu})$, the turbulence model is similarly stabilized by the SUPG method by adding the stabilizing term

$$B_{stab,S}|_{u}(\tilde{\nu}; m) := \sum_{K \in \mathcal{T}^h} (\tau_M r_S(\tilde{\nu}, u), u \cdot \nabla m)_K.$$

2.3. *Isogeometric discretization*

In isogeometric analysis, the computational domain is inherited directly from a CAD model of the embedded structure (such as a turbine blade). This relieves a part of the task of volume mesh generation, but does not obviate it entirely. The interior of the volume needs to be meshed in a way that retains control over the mesh quality and resolution, especially in the boundary layer and separation regions. A modified transfinite interpolation technique is used here, which is detailed in [15]. We merely discuss a few important features of the resulting meshes here. The mesh (i.e., the tesselation $\mathcal{T}^h$) has a tensorial structure and is isotropic, having exponential grading away from aerodynamic surfaces. Mesh quality in the boundary layer is safeguarded by extending mesh lines in the normal direction in the vicinity of the boundary. Fig. 1 shows how the linear approximation of the geometry of a typical airfoil section degrades the aerodynamic surface, and illustrates an advantage of the isogeometric approach.

The approximation spaces derive from the resulting geometrical description of the volume. As airfoil sections are typically defined by polynomials, we consider b-spline discretizations here as well. A concise introduction to this technology is given here, the interested reader is referred to [16] for an introduction to isogeometric analysis and to [17] for their implementation.

A b-spline basis is constructed from a tensor-product (patch in a) mesh, with associated knot-vectors corresponding to mesh lines in one direction $\Xi = \{\xi_i\}_{i \le n+p}$, where k is a parametric direction $\in \{0, 1\}$, n the number of elements in that direction and p the polynomial order in that direction. We consider the case that $\xi_i \neq \xi_j$ if $i \neq j$ and $p \le i, j \le n+1$, i.e. for an open knot interval with no repeated interior knots. A b-spline basis of polynomial order p is defined recursively through the Cox-de Boor formula:

$$\begin{aligned}
b_j^0(\xi) &:= \chi(\xi_j, \xi_{j+1}), \quad j \le n\\
b_j^p(\xi) &:= \frac{\xi - \xi_j}{\xi_{j+p} - \xi_j} b_j^{p-1}(\xi) + \frac{\xi_{j+p+1} - \xi}{\xi_{j+p+1} - \xi_{j+1}} b_{j+1}^{p-1}(\xi), \quad j \le n + p - 1
\end{aligned}$$

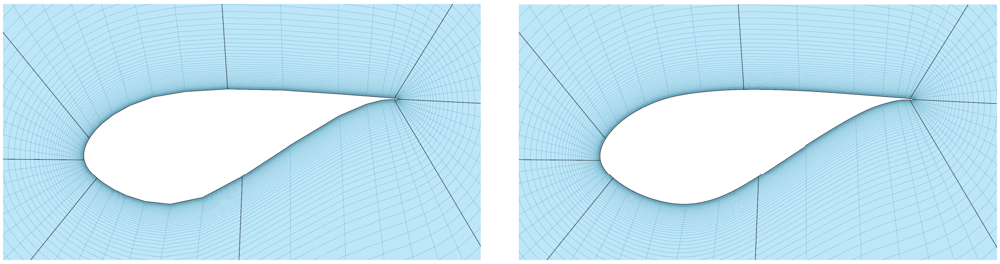

Fig. 1: Representation of a cross section of a blade using linear elements (left) and cubic splines (right).

with $\chi(a, b)$ the indicator function on (a, b). An ansatz function N_i^p is then constructed as a product of such univariate functions, one in each direction. The geometry, and any solution variable is then represented as a linear combination of such ansatz functions:

$$x(\boldsymbol{\xi}) = \Sigma_i \hat{\boldsymbol{x}}_i N_i^p(\boldsymbol{\xi}) \text{ and} p(\boldsymbol{\xi}) = \Sigma_i \hat{p}_i N_i^p(\boldsymbol{\xi}), \tag{5}$$

respectively. The b-spline basis $\{N_i^p\}_i$ has a number of properties important in this discussion:

1. N_i^p is a piecewise polynomial of degree p and possesses $p-1$ continuous derivatives, i.e., it is a member of $C^{p-1}(\Omega)$). So, if $p > 1$ the basis functions are smooth.
2. Increasing p (performing k-refinement) only mildly increases the number of degrees of freedom, $\#\{b_i^p\}_i = \#\{b_i^{p-1}\}_i + 1$, the cost of increasing p rather comes from matrix fill and quadrature.

The term *isogeometric analysis* has evolved into designating smooth (and not merely continuous) bases. The trilinear basis, with $p = 1$, is often called *traditional (lagrangian) finite elements*; whereas smoother representations with $p > 1$ are called isogeometric.

2.4. Time discretization

The second-order backward difference technique is used to resolve the time-derivative in B_{NS} and B_{SA} of (4). Thus, the solution is sought only at time levels $t_k = k\Delta t$, $k < T/\Delta t$. Denoting the solution variable at time level k as u_k, the difference formula reads $\partial_t u(t_k) = (3u_k - 4u_{k-1} + u_{k-2})/\left(2\Delta t^2\right) + O(\Delta t^2)$.

2.5. Solution techniques

The time-discretized version of (4) is solved in a partitioned way: for each time step Newton's method is applied first to the (v, q)-equation and then to the m-equation. The target applications are three-dimensional, time-dependent, high Reynolds number flows. Equation solving then quickly becomes a time-consuming task that is to be addressed by both parallelization and efficient preconditioners. We build on the MPI functionality and solvers in PETSc [18].

Efficient preconditioners for the discretized Navier-Stokes equations can be derived using the block structure of the linearized system which is assembled at each Newton iteration, written as:

$$\begin{bmatrix} F & B^\top \\ B & -C \end{bmatrix} \begin{Bmatrix} \hat{u} \\ \hat{p} \end{Bmatrix} = \begin{Bmatrix} \hat{f} \\ \hat{0} \end{Bmatrix},$$

where $\hat{u} = \{\hat{u}_i\}_i$ collects the velocity degrees of freedom defined in (5), similary $\hat{p}$ collects the pressure degrees of freedom. A block-diagonal preconditioner based on the Schur complement $S = -C - BF^{-1}B^\top$ is used. A sufficient approximation for F^{-1} is given by the SOR preconditioner. The Schur complement is first approximated by taking for F^{-1} the inverse of its diagonal (also called the SIMPLE method), and then using a multigrid or additive Schwarz method to approximate the inverse of the perturbed Schur complement. Then the system is solved with a Krylov method for asymmetric systems, e.g. GMRES. Concerning the m-equation, a similar approach to the velocity block is taken: an SOR preconditioner and a GMRES solver.

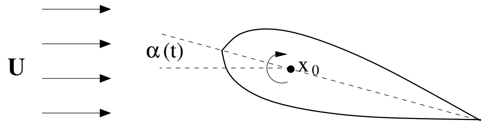

Fig. 2: Schematic of the problem setup for a pitching airfoil.

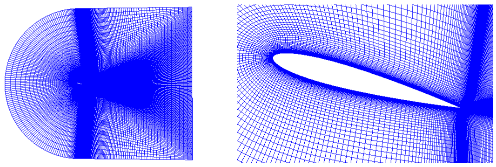

Fig. 3: C-mesh of the flow domain.

3. Pitching airfoil at Re=980 000

We consider here a narrow section of a wind turbine blade undergoing a prescribed motion. This problem simplifies but mimicks the intended application and allows comparison with experiments performed in [19]. We will investigate the gain an isogeometric approach yields.

A NACA 0015 airfoil oscillates around the quarter chord point, following a sinusoidal pitching motion: $\alpha(t) = 14.85° + 9.89°\sin(\omega t)$, see figure 2. A so-called C-mesh is constructed, as shown in fig. 3. The mesh consists of $5 \cdot 10^4$ elements with 200 elements along the wing surface. The wall-normal mesh size is $1 \cdot 10^{-5}$. A time step of $\Delta t = 1 \cdot 10^{-3}$ is chosen. The response is shown in figs. 4 and 5. In the first panel of fig. 4, the airfoil is in the neutral position and pitching up. The flow is largely attached. In the second panel, the pitch attains its maximum value and a large separation bubble causes low pressures along the upper side of the airfoil, causing high lift and drag. The lift is much higher than what would be expected in the stationary case, where the flow separates soon after $\alpha = 15°$. As this bubble travels downstream and reaches the trailing edge, the lift suddenly plunges, as can bee seen in the C_L plot of fig. 5. The third panel shows the separation bubble moving downstream. In the last panel, the airfoil reaches its minimum pitch, the transients have been transported downstream and the steady response is recovered.

It is clear that a good qualitative prediction can be made of the aerodynamic coefficients, although the SA model cannot capture the parts of the cycle with large recirculation regions. What is also observed is that in this setup the increase of the polynomial order has little gain, especially in the light of these large modeling errors.

4. Conclusions and future work

In this paper, an isogeometric ALE-RANS model with a Spalart-Almaras turbulence model was introduced as a flow simulator for the FSI of wind turbines. The additional value of using isogeometric analysis was investigated for a pitching airfoil at Re=$9.8 \cdot 10^5$. In this setting it is seen that the isogeometric and the traditional finite-element approach perform equally well when compared to experimental values. The turbulence modeling error is much larger than that of the discretization. This result complements other scenario's where the additional smoothness is seen to significantly improve results. These other scenario's include those where the Reynolds number is low [20], and those where more accurate turbulence models are used [4].

The 2D approach to modeling aerodynamic characteristics of a section of turbine blade can have applications in improving inputs to wake models utilized in mico and mesoscale simulations like the ones presented in [21]. The wake modeling in a realistic wind farm requires a database of the sectional geometry and aerodynamic coefficients of the operatinal turbines. So far standard geometries and coefficients are utilized in the simulations but the work presented in this paper will help in creating a turbine specific database. The accuracy is expected to improve even further with

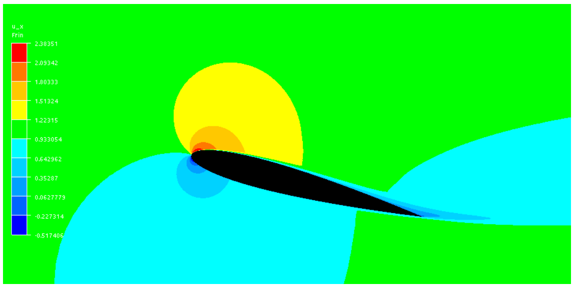

(a) $t = 0T$

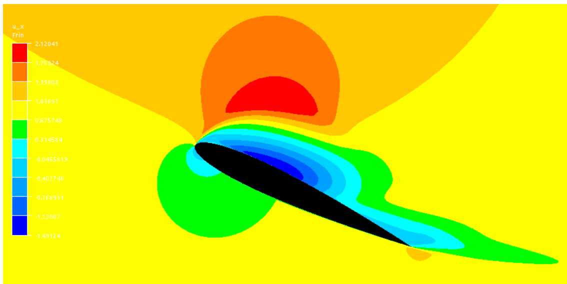

(b) $t = 0.25T$

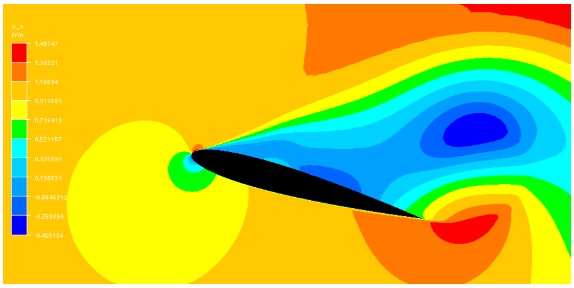

(c) $t = 0.5T$

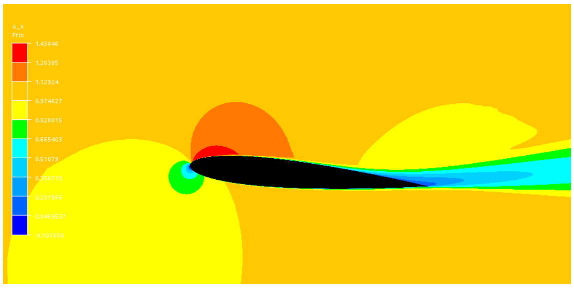

(d) $t = 0.75T$

Fig. 4: Snapshots of the horizontal velocity during different phases of the periodic cycle.

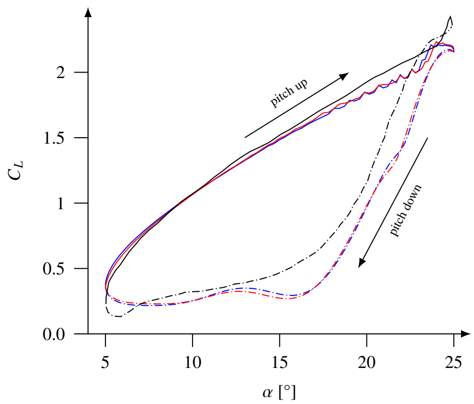

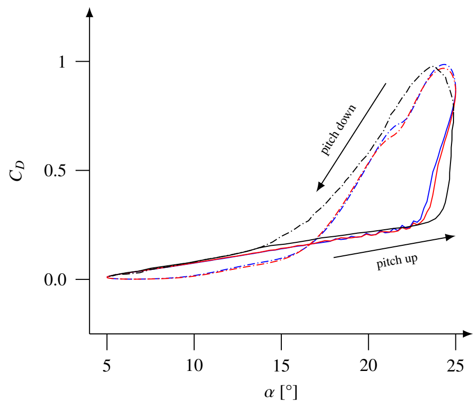

Fig. 5: Aerodynamic coefficients during a periodic cycle, with – experiments from [19], – $p = 1$ and – $p = 2$.

the extension of the current work to 3D ([22]) and then its integration to a beam model ([23]) for a realistic fluid structure interaction simulation.

Acknowledgements

The authors acknowledge the financial support from the Norwegian Research Council and the industrial partners of the FSI-WT (216465/E20) (`http://www.fsi-wt.no`) and NOWITECH: Norwegian Research Centre for Offshore Wind Technology (`http://www.nowitech.no`) projects.

References

[1] Bazilevs, Y., Hsu, M.C., Akkerman, I., Wright, S., Takizawa, K., Henicke, B., et al. 3D simulation of wind turbine rotors at full scale. part I: Geometry modeling and aerodynamics. International Journal for Numerical Methods in Fluids 2011;65(1-3):207–235. URL: http://dx.doi.org/10.1002/fld.2400. doi:10.1002/fld.2400.

[2] Bazilevs, Y., Hsu, M.C., Kiendl, J., Wüchner, R., Bletzinger, K.U.. 3D simulation of wind turbine rotors at full scale. part II: Fluid-structure interaction modeling with composite blades. International Journal for Numerical Methods in Fluids 2011;65:265–253.

[3] Hsu, M.C., Bazilevs, Y.. Fluid–structure interaction modeling of wind turbines: simulating the full machine. Computational Mechanics 2012;50:821–833.

[4] Bazilevs, Y., Michler, C., Calo, V., Hughes, T.. Weak dirichlet boundary conditions for wall-bounded turbulent flows. Computer Methods in Applied Mechanics and Engineering 2007;196:4853–4862.

[5] Nordanger, K., Holdahl, R., Kvarving, A., Rasheed, A., Kvamsdal, T.. Implementation and comparison of three isogeometric Navier-Stokes solvers applied to simulation of flow past a fixed 2D NACA0012 airfoil at high Reynolds number. Computer Methods in Applied Mechanics and Engineering 2014;Accepted.

[6] Nordanger, K., Kvamsdal, T., Kvarving, A., Mathisen, K., Okstad, K., Rasheed, A., et al. Strip theory approach for FSI-simulation of flow around turbine blades. In: EERA DeepWind 2015, 12^{12} Deep Sea Offshore Wind R&D Conference. 2015,.

[7] Collier, N., Dalcin, L., Pardo, D., Calo, V.. The cost of continuity: performance of iterative solvers on isogeometric finite elements. SIAM Journal on Scientific Computing 2013;35(2):A767–A784.

[8] Akkerman, I., Bazilevs, Y., Calo, V., Hughes, T., Hulshoff, S.. The role of continuity in residual-based variational multiscale modeling of turbulence. Computational Mechanics 2008;41:371–378.

[9] Evans, J., Hughes, T.. Isogeometric divergence-conforming B-splines for the unsteady Navier–Stokes equations. Journal of Computational Physics 2013;241:141–167.

[10] Johannessen, K., Kumar, M., Kvamsdal, T.. Divergence-conforming discretization for Stokes problem on locally refined meshes using LR B-splines. Computer Methods in Applied Mechanics and Engineering 2015;submitted.

[11] Spalart, P., Allmaras, S.. A one-equation turbulence model for aerodynamic flows. American Institute of Aeronautics and Astronautics Journal 1992;94-439.

[12] Allmaras, S., Johnson, F., Spalart, P.. Modifications and clarifications for the implementation of the spalart-allmaras turbulence model. In: VII Conference on CFD. 2012, p. 1–11.

[13] Brooks, A., Hughes, T.. Streamline upwind/Petrov-Galerkin formulations for convection dominated flows with particular emphasis on the incompressible Navier-Stokes equations. Computer Methods in Applied Mechanics and Engineering 1982;32:199–259.

[14] Hughes, T., Fanca, L., Balestra, M.. A new finite elment formulation for computational fluid dynamics: V. circumventing the Babuška-Brezzi condition: A stable Petrov-Galerkin formulation of the Stokes problem accomodating equal-order interpolations. Computer Methods in Applied Mechanics and Engineering 1986;59:85–99.

[15] Fonn, E., Rasheed, A., Kvarving, A., Kvamsdal, T., Tabib, M., Opstal, T.. Spline based mesh generator for high fidelity simulation of flow around turbine blades. In: EERA DeepWind 2015, 12^{12} Deep Sea Offshore Wind R&D Conference. 2015,.

[16] Hughes, T., Cottrell, J., Bazilevs, Y.. Isogeometric analysis: CAD, finite elements, NURBS, exact geometry and mesh refinement. Computational Methods in Applied Mechanics and Engineering 2005;194:4135–4195.

[17] Piegl, L., Tiller, W.. The NURBS Book. 2^{nd} ed.; Springer-Verlag; 1997.

[18] Balay, S., Abhyankar, S., Adams, M.F., Brown, J., Brune, P., Buschelman, K., et al. PETSc users manual. Tech. Rep. ANL-95/11 - Revision 3.5; Argonne National Laboratory; 2014. URL: http://www.mcs.anl.gov/petsc.

[19] McAlister, K., Takahashi, R.. Naca 0015 wing pressure and trailing vortex measurements. VSCOM technical report 91-A-003; NASA; 1991.

[20] Nordanger, K., Rasheed, A., Okstad, K.M., Kvarving, A.M., Holdahl, R., Kvamsdal, T.. Numerical benchmarking of fluid-structure interaction: An isogeometric finite element approach. Submitted to the Journal of Fluids and Structures 2015;.

[21] Tabib, M., Rasheed, A., Kvamsdal, T.. Investigation of the impact of wakes and stratification on the performance of an onshore wind farm. In: EERA DeepWind 2015, 12^{12} Deep Sea Offshore Wind R&D Conference. 2015,.

[22] Kvarving, A., Kvamsdal, T., Rasheed, A., Okstad, K., Fonn, E., Mathisen, K., et al. 3d cfd and fsi-simulation of flow around turbine blades. In: EERA DeepWind 2015, 12^{12} Deep Sea Offshore Wind R&D Conference. 2015,.

[23] Okstad, K., Mathisen, K., Kvamsdal, T., Kvarving, A., Nordanger, K., Rasheed, A., et al. 3d beam element for fsi-simulation of flow around turbine blades. In: EERA DeepWind 2015, 12^{12} Deep Sea Offshore Wind R&D Conference. 2015,.